

## EFFECTS OF WALL CURVATURE ON TURBULENT HEAT TRANSFER IN CURVED PIPE FLOW

**Changwoo Kang and Kyung-Soo Yang**  
Department of Mechanical Engineering,  
Inha University  
Incheon 402-751, Korea  
(TEL) 82 32 860 7322  
(FAX) 82 32 868 1716  
(E-mail) [ksyang@inha.ac.kr](mailto:ksyang@inha.ac.kr)

### ABSTRACT

Direct numerical simulation (DNS) of fully-developed turbulent curved pipe flow has been performed to investigate the effects of wall curvature on turbulent flow and heat transfer. We consider a fully developed turbulent curved pipe flow with axially uniform wall heat flux. The Reynolds number under consideration is  $Re_\tau=210$  based on the mean friction velocity and the pipe radius, and the Prandtl number is 0.71. The mean velocity profiles and turbulent intensities obtained from the present DNS are in good agreement with the previous numerical and experimental results currently available. The mean quantities and various turbulence statistics are presented for flow and temperature fields.

### INTRODUCTION

Turbulent pipe flow has been attracting researchers' attention for decades due to its high applicability to many engineering devices such as heat exchangers, chemical reactors, power-plant piping systems, to name a few. In particular, turbulent characteristics of fluid flow and heat transfer have been intensively studied because complete understanding of them can lead to a significant improvement of transport efficiency in such devices, or to an effective way of reducing flow-accelerated erosion-corrosion (Enayet et al., 1982; Sudo et al., 1998, 2000).

A large volume of work on turbulent straight-pipe flow can be found in the literature, including numerical as well as experimental studies. Most of the numerical investigations were carried out by Direct Numerical Simulation (DNS) or Large Eddy Simulation (LES), and some reliable data bases were obtained (Unger and Friedrich, 1991; Eggels et al., 1994; den Toonder and Nieuwstadt, 1997; Wagner et al., 2001; Feiz et al., 2003; Wu and Moin, 2008). However, that was not the case for turbulent curved-pipe flow even though curved parts are widely used in a modern piping system to save space and also to enhance scalar transport via the secondary flows incurred by the wall curvature.

In the past, studies on curved-pipe flow were mainly done by experiments (Adler, 1934; Ito, 1959; Mori and Nakayama, 1965) or by theoretical analysis (Collins and Dennis, 1975; Wang, 1981; Dennis and Ng, 1982;

Germano, 1982, 1989). One can refer to Berger et al. (1983) and Ito (1987) for an extensive review on the subject. Recently, more attention has been paid to turbulent flow in a curved pipe, and detailed experimental measurements (Webster and Humphrey, 1993, 1997) as well as full three-dimensional (3D) simulations using DNS/LES (Boersma and Nieuwstadt, 1996; Boersma, 1997) have been performed. Hüttl et al. (1999) studied the effects of wall curvature on laminar pipe flow by using 3D simulation, and subsequently Hüttl and Friedrich (2000, 2001) compared their DNS results on the average velocity and velocity fluctuations in the fully developed curved-pipe flow at  $Re_\tau=230$  with those in the straight-pipe flow.

As far as heat/mass transfer in curved-pipe flow is concerned, research has been focused on the effects of the secondary flows induced by the wall curvature on the scalar transport. Mori and Nakayama (1965, 1967, 1967) theoretically computed resistance coefficients and heat transfer coefficients in laminar and turbulent curved-pipe flows, and showed that their results are well consistent with the experimental measurements (Pratt, 1947; Martinelli, 1947; Seban and McLaughlin, 1963; Rogers and Mayhew, 1964). Most of the following numerical investigations (Akiyama and Cheng, 1971; Kalb and Seader, 1972, 1974; Patankar et al., 1974; Yao and Berger, 1978; Zapryanov et al., 1980; Prusa and Yao, 1982), however, mainly studied correlation between Re (or Pr) and heat transfer rate. To the authors' best knowledge, in-depth studies on turbulence statistics of near-wall scalar fluctuations are rare. They are believed to significantly affect local heat/mass transfer rates on the pipe wall. The aims of the current investigation are to elucidate the near-wall characteristics of turbulent heat transfer in fully-developed curved-pipe flow by using DNS, and also to identify the curvature effects on the momentum and scalar transports by comparing our results with those of turbulent straight-pipe flow.

### GOVERNING EQUATIONS

The coordinate system used in the current study, a toroidal system, is presented in Fig. 1. As suggested by Wang (1981) and Germano (1982, 1989), an orthogonal curvilinear coordinate system is introduced in conjunction with a Cartesian coordinate system. By using the

curvilinear coordinates,  $r$  for the radial direction,  $\theta$  for the circumferential direction and  $s$  for the axial direction, a Cartesian position vector  $\mathbf{x}$  can be expressed as

$$\mathbf{x} = \mathbf{P} - \mathbf{O} = \mathbf{R}(s) + r \cos \theta \mathbf{N}(s) + r \sin \theta \mathbf{B}(s) \quad (1)$$

where  $\mathbf{R}$  represents a local point on the center curve.  $\mathbf{T}$ ,  $\mathbf{N}$  and  $\mathbf{B}$  are the tangential, normal, and binormal unit vectors. Using the relations

$$\mathbf{T} = \frac{d\mathbf{R}}{ds}, \quad \mathbf{N} = \frac{1}{\kappa} \frac{d\mathbf{T}}{ds}, \quad \mathbf{B} = \mathbf{T} \times \mathbf{N}, \quad \frac{d\mathbf{N}}{ds} = -\kappa \mathbf{T} \quad (2)$$

where  $\kappa$  is the curvature, the orthogonal metric of this system is given by

$$d\mathbf{x} \cdot d\mathbf{x} = dr^2 + (rd\theta)^2 + (1 + \kappa r \cos \theta)^2 ds^2 \quad (3)$$

where  $dr$ ,  $d\theta$ ,  $ds$  are the infinitesimal increments in the radial, circumferential and axial directions, respectively. With this metric, one can obtain the scale factors  $h_r$ ,  $h_\theta$  and  $h_s$ , (Batchelor, 1970)

$$h_r = 1, \quad h_\theta = r, \quad h_s = 1 + \kappa r \cos \theta \quad (4)$$

With these scale factors we can derive the continuity, momentum and energy equations in a conservative form. The governing incompressible continuity, momentum and energy equations turned out to be as follows (Boersma, 1997; Kalb and Seader, 1972) :

*Continuity equation:*

$$\frac{\partial}{\partial r}(rh_s u_r) + \frac{\partial}{\partial \theta}(h_s u_\theta) + \frac{\partial}{\partial s}(ru_s) = 0 \quad (5)$$

*r-momentum:*

$$\begin{aligned} \frac{\partial u_r}{\partial t} + \frac{1}{rh_s} \left( \frac{\partial}{\partial r}(rh_s u_r u_r) + \frac{\partial}{\partial \theta}(h_s u_\theta u_r) + \frac{\partial}{\partial s}(ru_s u_r) \right) - \frac{u_\theta u_\theta}{r} - \frac{u_s^2 \kappa \cos \theta}{h_s} \\ = \frac{1}{\rho} \frac{\partial p}{\partial r} + \frac{1}{rh_s} \left( \frac{\partial}{\partial r}(rh_s \tau_{rr}) + \frac{\partial}{\partial \theta}(h_s \tau_{r\theta}) + \frac{\partial}{\partial s}(r\tau_{rs}) \right) \\ - \frac{\tau_{\theta\theta}}{r} - \frac{\tau_{ss} \kappa \cos \theta}{h_s} \end{aligned} \quad (6)$$

*$\theta$ -momentum:*

$$\begin{aligned} \frac{\partial u_\theta}{\partial t} + \frac{1}{rh_s} \left( \frac{\partial}{\partial r}(rh_s u_r u_\theta) + \frac{\partial}{\partial \theta}(h_s u_\theta u_\theta) + \frac{\partial}{\partial s}(ru_s u_\theta) \right) + \frac{u_r u_\theta}{r} + \frac{u_s^2 \kappa \sin \theta}{h_s} \\ = \frac{1}{\rho r} \frac{\partial p}{\partial \theta} + \frac{1}{rh_s} \left( \frac{\partial}{\partial r}(rh_s \tau_{r\theta}) + \frac{\partial}{\partial \theta}(h_s \tau_{\theta\theta}) + \frac{\partial}{\partial s}(r\tau_{\theta s}) \right) \\ + \frac{\tau_{r\theta}}{r} + \frac{\tau_{ss} \kappa \sin \theta}{h_s} \end{aligned} \quad (7)$$

*s-momentum:*

$$\begin{aligned} \frac{\partial u_s}{\partial t} + \frac{1}{rh_s} \left( \frac{\partial}{\partial r}(rh_s u_r u_s) + \frac{\partial}{\partial \theta}(h_s u_\theta u_s) + \frac{\partial}{\partial s}(ru_s u_s) \right) + \frac{u_r \kappa}{h_s} (u_r \cos \theta - u_\theta \sin \theta) \\ = \frac{1}{\rho h_s} \frac{\partial p}{\partial s} + \frac{1}{rh_s} \left( \frac{\partial}{\partial r}(rh_s \tau_{rs}) + \frac{\partial}{\partial \theta}(h_s \tau_{\theta s}) + \frac{\partial}{\partial s}(r\tau_{ss}) \right) \end{aligned}$$

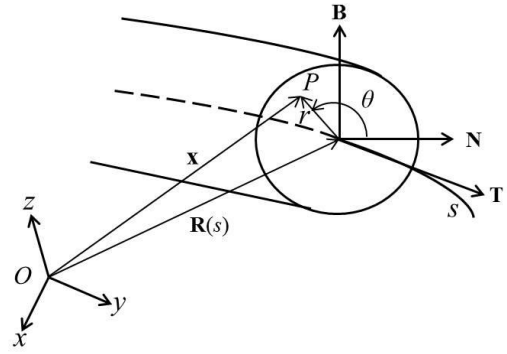


Figure 1. Coordinate system.

$$+ \frac{\tau_{rs} \kappa \cos \theta}{h_s} - \frac{\tau_{\theta s} \kappa \sin \theta}{h_s} \quad (8)$$

*Energy equation:*

$$\begin{aligned} \frac{\partial T}{\partial t} + \frac{1}{rh_s} \left( \frac{\partial}{\partial r}(rh_s u_r T) + \frac{\partial}{\partial \theta}(h_s u_\theta T) + \frac{\partial}{\partial s}(ru_s T) \right) \\ = \frac{\alpha}{rh_s} \left( \frac{\partial}{\partial r} \left( rh_s \frac{\partial T}{\partial r} \right) + \frac{\partial}{\partial \theta} \left( \frac{h_s}{r} \frac{\partial T}{\partial \theta} \right) + \frac{\partial}{\partial s} \left( \frac{r}{h_s} \frac{\partial T}{\partial s} \right) \right) \end{aligned} \quad (9)$$

Here,  $\rho$ ,  $p$ ,  $v$ ,  $\alpha$  represent density, pressure, kinematic viscosity, and thermal diffusivity of the fluid, respectively.  $\tau_{ij}$  is the symmetric viscous stress tensor with the following components

$$\begin{aligned} \tau_{rr} = v \left( 2 \frac{\partial u_r}{\partial r} \right), \quad \tau_{r\theta} = v \left( \frac{1}{r} \frac{\partial u_r}{\partial \theta} + r \frac{\partial}{\partial r} \left( \frac{u_\theta}{r} \right) \right), \quad \tau_{rs} = v \left( \frac{1}{h_s} \frac{\partial u_r}{\partial s} + h_s \frac{\partial}{\partial r} \left( \frac{u_s}{h_s} \right) \right), \\ \tau_{\theta\theta} = v \left( 2 \left( \frac{u_r}{r} + \frac{1}{r} \frac{\partial u_\theta}{\partial \theta} \right) \right), \quad \tau_{\theta s} = v \left( \frac{r}{h_s} \frac{\partial}{\partial s} \left( \frac{u_\theta}{r} \right) + \frac{h_s}{r} \frac{\partial}{\partial \theta} \left( \frac{u_s}{h_s} \right) \right), \\ \tau_{ss} = v \left( 2 \left( \frac{u_r \kappa \cos \theta}{h_s} - \frac{u_\theta \kappa \sin \theta}{h_s} + \frac{1}{h_s} \frac{\partial u_s}{\partial s} \right) \right) \end{aligned} \quad (10)$$

## NUMERICAL METHODS AND BOUNDARY CONDITION

The governing equations (Eqs. (5) ~ (9)) were discretized by using a finite volume method. All the physical variables were non-dimensionalized with the pipe radius ( $a$ ), mean friction velocity ( $u_\tau$ ), and mean friction temperature ( $T_\tau = q_w / \alpha / u_\tau$ ). Here,  $q_w$  is the wall heat flux that is constant. The mean friction velocity ( $u_\tau$ ) is defined as follows (Boersma, 1996; Hüttel and Friedrich, 2000, 2001) :

$$u_\tau = \frac{1}{2\pi} \left( \int_0^{2\pi} u_\tau^2(\theta) d\theta \right)^{1/2} \quad (11)$$

A second-order central difference scheme was used for spatial discretization. A hybrid scheme was employed for time advancement. In particular, following Akselvoll and Moin (1996), we partitioned the  $r$ - $\theta$  domain into the core region ( $0 \leq r \leq r_c$ ) and the outer region ( $r \geq r_c$ ). Here,  $r_c$  is the boundary between the two regions, and we set

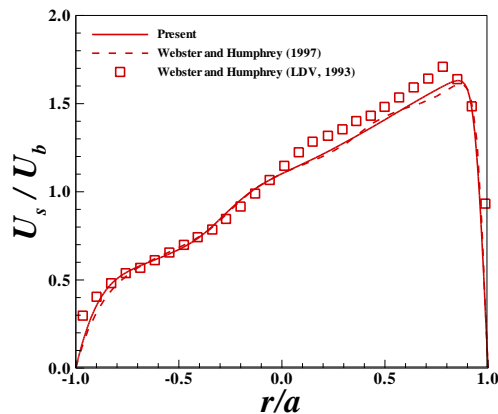


Figure 2. Mean axial velocity profiles along a horizontal line for  $Re_b=5480$ ,  $\kappa=1/18.2$ .

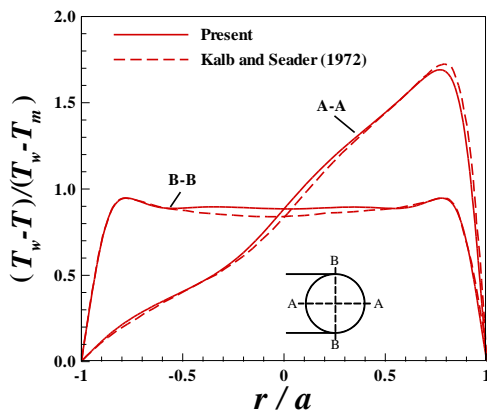


Figure 3. Temperature profiles for  $K=512$ ,  $\kappa=1/15.2$ ,  $Pr=0.7$ .

$r_c=0.5a$ . In the core region, both the convective and diffusion terms are implicitly time-advanced only in the circumferential direction, while the other terms are explicitly advanced. On the other hand, in the outer region, the convective and diffusion terms are implicitly treated only in the radial direction, and the other terms are explicitly advanced. In both regions, the Crank-Nicolson method was employed as the implicit scheme, while a third-order Runge-Kutta method was used as the explicit scheme. To decouple the continuity and momentum equations, a fractional step method was used (Kim and Moin, 1985).

The no-slip condition was imposed on the pipe wall, while flow was assumed to be periodic in the axial direction. For the temperature boundary conditions, heat flux ( $q_w$ ) was set constant on the pipe wall, and it was assumed that the temperature field is periodic in the axial direction (Kalb and Seader, 1972; Patankar et al., 1977).

The flow is driven in the axial direction by a mean pressure gradient  $\Delta p/\Delta s$ , which must balance the viscous friction along the pipe wall and can be estimated from a simple force equilibrium (Boersma and Nieuwstadt, 1996)

$$\frac{\Delta p}{\Delta s} = -\frac{4\rho u_\tau^2}{D} \quad (12)$$

where  $D$  and  $\Delta s$  represent the pipe diameter ( $2a$ ) and a distance along the pipe centerline, respectively.

## COMPUTATIONAL DETAILS

The pipe length along the axial coordinate  $s$  is taken to be  $15a$ . The Reynolds number ( $Re_\tau$ ) considered here is 210 based on the pipe radius ( $a$ ) and the mean friction velocity ( $u_\tau$ ), whereas the Prandtl number ( $Pr$ ) is 0.71. The curvature ( $\kappa$ ) is  $1/18.2$ . The numerical resolution was determined by a grid refinement study. The number of grid cells used in the current investigation was  $96(r) \times 192(\theta) \times 256(s)$ . A uniform grid was used in  $\theta$  and  $s$  directions. In the wall-normal radial direction, grid points were clustered close to the wall. (Boersma, 1997; Hüttel and Friedrich, 2000, 2001)

## VALIDATION

To validate our code, our results are compared against those of other authors currently available. In Fig. 2, the mean axial velocity profile along a wall-normal radial line on the symmetric plane is presented, when the Reynolds number ( $Re_b$ ) equals 5,480 with  $\kappa=1/18.2$ . Here, the Reynolds number,  $Re_b(=U_b D/\nu)$ , is defined based on the axial mean bulk velocity ( $U_b$ ) and the pipe diameter ( $D$ ). The experimental result (LDV) of Webster and Humphrey (1993) and the DNS result of Webster and Humphrey (1997) are also shown together. Our result is in good agreement with theirs.

Fig. 3 presents the nondimensionalized temperature profiles along the lines A-A and B-B for  $K=512$ ,  $\kappa=1/15.2$ ,  $Pr=0.7$  in comparison with the numerical simulation of Kalb and Seader (1972). Here,  $T_m$  and  $T_w$  represent mean bulk temperature and wall temperature, respectively. The Dean number ( $K=Re_b\sqrt{\kappa}$ ) is set as  $K=512$ . The two results are in good agreement. It is also seen that the temperature profile on A-A very much resembles the axial velocity profile shown in Fig. 2.

## RESULTS

Fig. 4 shows the mean axial velocity profiles along the horizontal line (A-A) and vertical line (B-B) for  $Re_\tau=210$ ,  $\kappa=1/18.2$ . Due to the curvature effect, the peak is shifted towards the outer wall ( $r/a=1$ ) along A-A, whereas the profile is symmetric with respect to  $r/a=0$  along B-B. It is also seen that both the mean axial velocity and its gradient in the immediate vicinity of the outer wall are larger than those very near the inner wall ( $r/a=-1$ ). However, the profile of mean axial velocity along the vertical line (B-B) is symmetric with respect to the center plane, and has the maximum points near the outer as well as the inner walls.

Figure 5 presents the profiles of nondimensionalized mean temperature ( $T^+ = (T_w - T)/T_\tau$ ) on the horizontal line (A-A) and on the vertical line (B-B). Here,  $T_w$  denotes wall temperature. The mean temperature distributions on the two lines closely follow those of the mean axial velocity component (Fig. 4). It is seen in Fig. 5 that the mean temperature gradient on the outer wall ( $r/a=1$ ) is steeper than that on the inner wall ( $r/a=-1$ ) on the

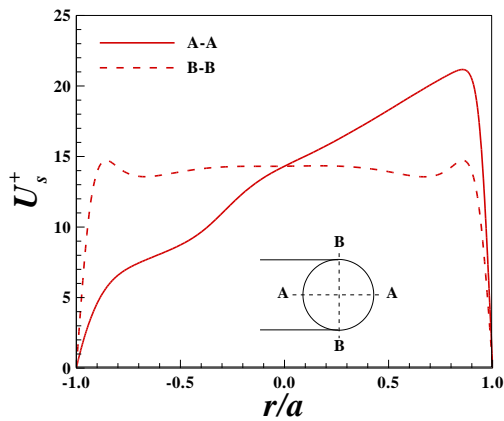


Figure 4. Profiles of mean axial velocity component,  $Re_\tau=210$ ,  $\kappa=1/18.2$ .

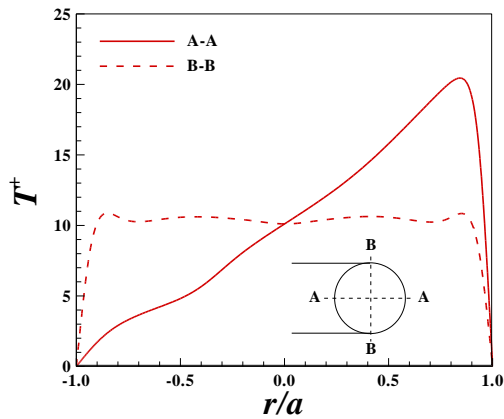


Figure 5. Mean temperature profiles,  $Re_\tau=210$ ,  $\kappa=1/18.2$ ,  $Pr=0.71$ .

horizontal line (A-A). This indicates, from the viewpoint of local heat transfer rate, that the curvature enhances heat transfer on the outer wall, but that is not the case on the inner wall. On the other hand, for the curved pipe flows, the mean temperature is almost constant along the central part of the vertical line (B-B).

Distributions of mean velocity and temperature fields are depicted on an  $r-\theta$  plane in Fig. 6. Contours of the axial velocity component are presented in Fig. 6(a). The high-velocity region is shifted towards the outer wall due to the curvature, but still symmetric with respect to the horizontal line. It is also noticed that in the central region, the contours are almost perpendicular to the horizontal line. Contours of nondimensionalized mean temperature are shown on a  $r-\theta$  plane in Fig. 6(b). As also seen in Fig. 5, the high-temperature region is shifted towards the outer wall due to the curvature effect, and the mean temperature is almost constant in the vertical direction in the central region. The secondary flows are clearly seen in Figs. 6(c)-6(d) that presents the velocity vectors and streamlines, respectively, on an  $r-\theta$  plane. The centrifugal force is mainly balanced by the pressure gradient. Since the axial momentum near the pipe wall is very small, the balance is broken, resulting in movement of fluid particles towards the inner wall. Consequently, fluid particles near the inner

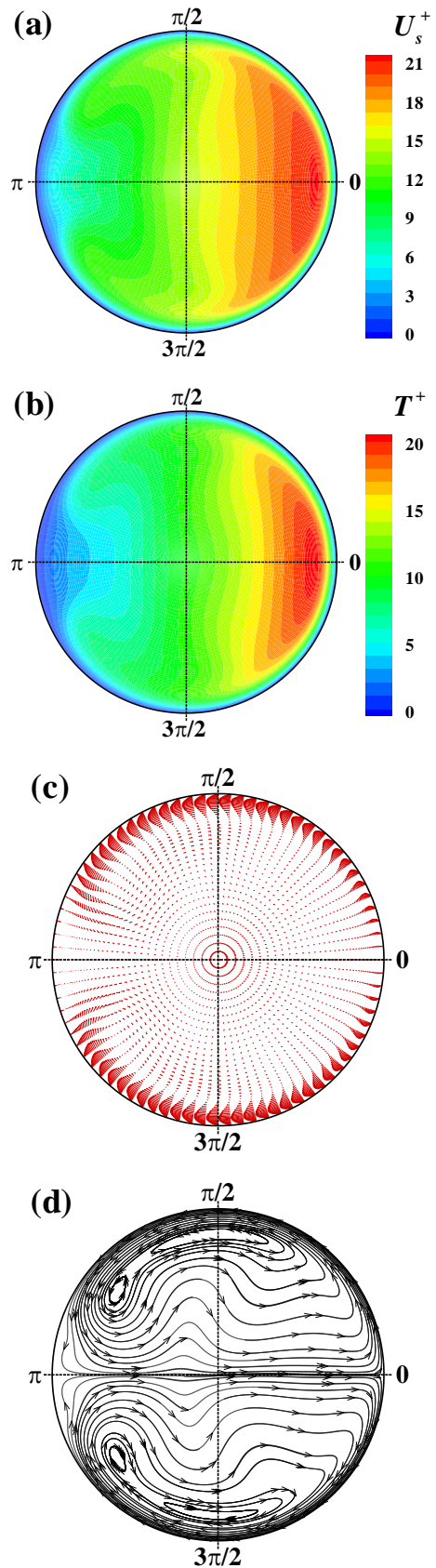


Figure 6. Secondary flow in an  $r-\theta$  plane; (a) mean axial velocity contour, (b) nondimensionalized mean temperature contour, (c) velocity vector plot, (d) streamlines.

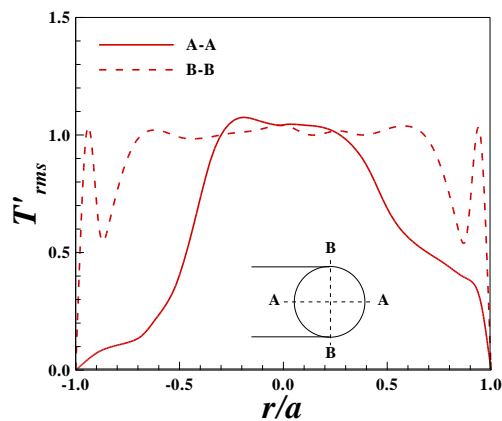


Figure 7. Profiles of root-mean-square of the temperature fluctuation,  $Re_{\tau}=210$ ,  $\kappa=1/18.2$ ,  $Pr=0.71$ .

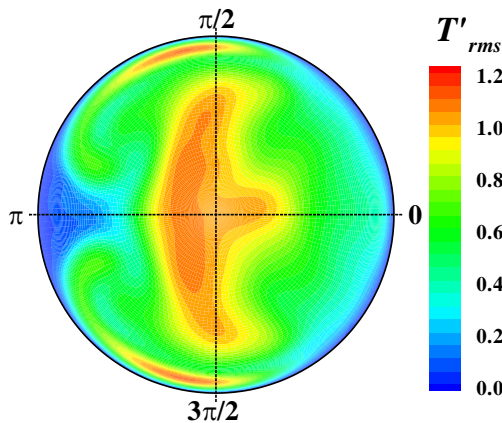


Figure 8. Contours of rms of the temperature fluctuation in an  $r$ - $\theta$  plane,  $Re_{\tau}=210$ ,  $\kappa=1/18.2$ ,  $Pr=0.71$ .

wall are driven towards the outer wall due to continuity, forming a pair of counter-rotating and symmetric secondary flows. Therefore, a stagnation point is formed at each end of the horizontal line (A-A), and significant circumferential velocity is induced near the pipe wall.

Figure 7 shows profiles of the temperature fluctuation rms along the horizontal line (A-A) and vertical line (B-B). Like the mean temperature profile on A-A in Fig. 5, both rms value and its gradient are larger near the outer wall ( $r/a=1$ ) than near the inner wall ( $r/a=-1$ ). On the vertical line (B-B), both rms value and its gradient are large near both ends. Figure 8 presents contours of temperature fluctuation rms in an  $r$ - $\theta$  plane, confirming that rms is large in the central region as well as near the upper and lower walls.

## CONCLUSION

Direct numerical simulation of fully-developed turbulent curved pipe flow has been performed to study the effects of the pipe curvature on the characteristics of flow structures and heat transfer. The parameters were set as  $Re_{\tau}=210$ ,  $Pr=0.71$ , and  $\kappa=1/18.2$ . The curvature induces a pair of counter-rotating secondary flows on a cross-

section, and the high-velocity region is shifted towards the outer wall. Furthermore, the mean axial velocity component is almost constant in the vertical direction in the central region of the pipe. The mean temperature distribution on a cross-section is remarkably similar to that of the mean axial velocity component. Rms of temperature fluctuation is large in the central region as well as near the upper and lower walls.

## ACKNOWLEDGEMENT

This work was supported by the National Research Foundation of Korea (NRF) grant funded by the Korea government (MEST) (No. 2012R1A2A2A01013019).

## REFERENCES

- Adler, M., 1934, "Strömung in gekrümmten Röhren", *Zeitschrift für angewandte Mathematik und Mechanik*, Vol. 14, pp. 257-275.
- Akiyama, M., and Cheng, K. C., 1971, "Boundary vorticity method for laminar forced convection heat transfer in curved pipes", *Int. J. Heat Mass Transfer*, Vol. 14, pp. 1659-1675.
- Akselvoll, K., and Moin, P., 1996, "An efficient method for temporal integration of the Navier-Stokes equation in confined axisymmetric geometries", *J. Comput. Phys.*, Vol. 125, pp. 454-463.
- Batchelor, G. K., 1970, *An Introduction to Fluid Mechanics*, Appendix 2, Cambridge University Press.
- Berger, S. A., Talbot, L., and Yao, L. -S., 1983, "Flow in curved pipe", *Ann. Rev. Fluid Mech.*, Vol. 15, pp. 461-512.
- Boersma, B. J., and Nieuwstadt, F. T. M., 1996, "Large-eddy simulation of turbulent flow in a curved pipe", *ASME J. Fluids Eng.*, Vol. 118, pp. 248-254.
- Boersma, B. J., 1997, *Electromagnetic effects in cylindrical pipe flow*, Ph.D. Thesis, Delft University Press.
- Collins, W. M., and Dennis, S. C. R., 1975, "The steady motion of a viscous fluid in a curved tube", *Q. J. Mech. Appl. Math.*, Vol. 28, pp. 133-156.
- Dennis, S. C. R., and Ng, M., 1982, "Dual solutions for steady laminar flow through a curved tube", *Q. J. Mech. Appl. Math.*, Vol. 35, pp. 305-324.
- den Toonder, J. M. J., and Nieuwstadt, F. T. M., 1997, "Reynolds number effects in a turbulent pipe flow for low to moderate  $Re$ ", *Phys. Fluids*, Vol. 9(11), pp. 3398-3409.
- Eggels, J. G. M., Unger, F., Weiss, M. H., Westerweel, J., Adrian, R. J., Friedrich, R., and Nieuwstadt, F. T. M., 1994, "Fully developed turbulent pipe flow : a comparison between direct numerical simulation and experiment", *J. Fluid Mech.*, Vol. 268, pp. 175-209.
- Enayet, M. M., Gibson, M. M., Taylor, M. K. P., and Yianneskis, M., 1982, "Laser-Doppler measurements of laminar and turbulent flow in a pipe bend", *Int. J. Heat Fluid Flow*, Vol. 3(4), pp. 213-219.
- Feiz, A. A., Ould-Rouis, M., and Lauriat, G., 2003, "Large eddy simulation of turbulent flow in a rotating pipe", *Int. J. Heat Fluid Flow*, Vol. 24(3), pp. 412-420.
- Germano, M., 1982, "On the effect of torsion on a helical pipe flow", *J. Fluid Mech.*, Vol. 125, pp. 1-8.

- Germano, M., 1989, "The Dean equations extended to a helical pipe flow", *J. Fluid Mech.*, Vol. 203, pp. 289-305.
- Hüttl, T. J., Wagner, C., and Friedrich, R., 1999, "Navier-Stokes solutions of laminar flows based on orthogonal helical coordinates", *Int. J. Numer. Meth. Fluids*, Vol. 29, pp. 749-763.
- Hüttl, T. J., and Friedrich, R., 2000, "Influence of curvature and torsion on turbulent flow in helically coiled pipes", *Int. J. Heat Fluid Flow*, Vol. 21, pp. 345-353.
- Hüttl, T. J., and Friedrich, R., 2001, "Direct numerical simulation of turbulent flows in curved and helically coiled pipes", *Comput. Fluids*, Vol. 30, pp. 591-605.
- Ito, H., 1959, "Friction factors for turbulent flow in curved pipes", *J. Basic Eng.*, Vol. 81, pp. 123-134.
- Ito, H., 1987, "Flow in curved pipes", *JSME Int. J.*, Vol. 30, pp. 543-552.
- Kalb, C. E., and Seader, J. D., 1972, "Heat and mass transfer phenomena for viscous flow in curved circular tubes", *Int. J. Heat Mass Transfer*, Vol. 15, pp. 801-817.
- Kalb, C. E., and Seader, J. D., 1974, "Fully developed viscous-flow heat transfer in curved circular tubes with uniform wall temperature", *AIChE J.*, Vol. 20(2), pp. 340-346.
- Kim, J. and Moin, P., 1985, "Application of a fractional-step method to incompressible Navier-Stokes equations", *J. Comput. Phys.*, Vol. 59, pp. 308-323.
- Martinelli, R. C., 1947, "Heat transfer to molten metals", *Trans. Am. Soc. Mech. Engrs.*, Vol. 69, pp. 947-959.
- Mori, Y., and Nakayama, W., 1965, "Study on forced convective heat transfer in curved pipes (1st Report, Laminar region)", *Int. J. Heat Mass Transfer*, Vol. 8, pp. 67-82.
- Mori, Y., and Nakayama, W., 1967, "Study on forced convective heat transfer in curved pipes (2nd Report, Turbulent region)", *Int. J. Heat Mass Transfer*, Vol. 10, pp. 37-59.
- Mori, Y., and Nakayama, W., 1967, "Study on forced convective heat transfer in curved pipes (3rd Report, Theoretical analysis under the condition of uniform wall temperature and practical formulae)", *Int. J. Heat Mass Transfer*, Vol. 10, pp. 681-695.
- Patankar, S. V., Pratap, V. S., and Spalding, D. B., 1974, "Prediction of laminar flow and heat transfer in helically coiled pipes", *J. Fluid Mech.*, Vol. 62, pp. 539-551.
- Patankar, S. V., Liu, C. H., and Sparrow, E. M., 1977, "Fully developed flow and heat transfer in ducts having streamwise-periodic variations of cross-sectional area", *ASME J. Heat Transfer*, Vol. 99, pp.180-186.
- Pratt, N. H., 1947, "The heat transfer in a reaction tank cooled by means of a coil", *Trans. Inst. Chem. Eng.*, Vol. 25, pp. 163-180.
- Prusa, J., and Yao, L. S., 1982, "Numerical solution for fully developed flow in heated curved tubes", *J. Fluid Mech.*, Vol. 123, pp. 503-522.
- Rogers, G. F. C., and Mayhew, Y. R., 1964, "Heat transfer and pressure loss in helically coiled tubes with turbulent flow", *Int. J. Heat Mass Transfer*, Vol. 7(11), pp. 1207-1216.
- Seban, R. A., and McLaughlin, E. F., 1963, "Heat transfer in tube coils with laminar and turbulent flow", *Int. J. Heat Mass Transfer*, Vol. 6(5), pp. 387-395.
- Sudo, K., Sumida, M., and Hibara, H., 1998, "Experimental investigation on turbulent flow in a circular-sectioned 90-degree bend", *Exp. Fluids*, Vol. 25, pp. 42-49.
- Sudo, K., Sumida, M., and Hibara, H., 2000, "Experimental investigation on turbulent flow through a circular-sectioned 180° bend", *Exp. Fluids*, Vol. 28, pp. 51-57.
- Unger, F., and Friedrich, R., 1991, "Large eddy simulation of fully-developed turbulent pipe flow", *Proc. 8th Symp. on Turbulent Shear Flows*, Munich, Germany.
- Wagner, C., Hüttl, T. J., and Friedrich, R., 2001, "Low-Reynolds-number effects derived from direct numerical simulations of turbulent pipe flow", *Comput. Fluids*, Vol. 30, pp. 581-590.
- Wang, C. Y., 1981, "On the low-Reynolds-number flow in a helical pipe", *J. Fluid Mech.*, Vol. 108, pp. 185-194.
- Webster, D. R., and Humphrey, J. A. C., 1993, "Experimental observations of flow instability in a helical coil", *ASME J. Fluids Eng.*, Vol. 115, pp. 436-443.
- Webster, D. R., and Humphrey, J. A. C., 1997, "Traveling wave instability in helical coil flow", *Phys. Fluids*, Vol. 9(2), pp. 407-418.
- Wu, X., and Moin, P., 2008, "A direct numerical simulation study on the mean velocity characteristics in turbulent pipe flow", *J. Fluid Mech.*, Vol. 608, pp. 81-112.
- Yao, L. -S., and Berger, S. A., 1978, "Flow in heated curved pipes", *J. Fluid Mech.*, Vol. 88, pp. 339-354.
- Zapryanov, Z., Christov, C., and Toshev, E., 1980, "Fully developed laminar flow and heat transfer in curved tubes", *Int. J. Heat Mass Transfer*, Vol. 23, pp. 873-880.